

A HF approach to La_2CuO_4 properties: hints for matching the Mott and Slater pictures

Alejandro Cabo-Bizet* and Alejandro Cabo-Montes de Oca**

**Departamento de Física, Centro de Aplicaciones Tecnológicas y Desarrollo Nuclear (CEADEN), Calle 30, esq. a 5ta, La Habana, Cuba. and*

***Grupo de Física Teórica, Instituto de Cibernética Matemática y Física (ICIMAF), Calle E, No. 309, entre 13 y 15, Vedado, La Habana, Cuba.*

(Dated: September 28, 2008)

It is argued that a Hartree-Fock (HF) solution for Coulomb interacting electrons in a simple model of the Cu-O planes in La_2CuO_4 , is able to predict some of the most interesting properties of this material, such as its insulator character and the antiferromagnetic order. Moreover, the natural appearance of pseudogaps in their paramagnetic and superconductor phases are also suggested by the discussion. These results follow after the elimination of some symmetry restrictions which are usually imposed on the single particle HF orbitals. One of them is the simplification of their spinor dependence to be of the so called α or β types. This constraint, seems to strongly reduce the largest space of orbitals corresponding to the rotational invariant HF formulation originally introduced by Dirac. We also remove, the demand on the HF orbitals of having a Bloch structure in the Bravais lattice of the crystal. This procedure allows for the consideration of HF solutions having the same symmetry than the known (symmetry breaking) antiferromagnetic structure of the material. It turns out that the most stable HF solution of the problem corresponds to an antiferromagnetic and insulating state (IAF), which magnetization rests on the experimentally determined direction. Encouragingly, the evaluated magnetic moment per cell is $0.67 \mu_B$, a result that satisfactorily reproduces the experimentally measured value: $0.68 \mu_B$. Another HF solution having a slightly higher energy arises and corresponds to a paramagnetic state showing a pseudogap (PPG). It follows after only imposing the Bloch structure on the single particle states. Finally a third paramagnetic but metallic solution (no gap) is also obtained by including both of the mentioned restrictions. The interesting result follows that this state only differs from the PPG pseudogap state in the form of excited empty orbitals. That is, the occupied single particle states and the HF energy at $T = 0$ for both solutions, are identical. In general, the discussion helps to clarify the role of the antiferromagnetic correlations in the structure of the physics of the HTSC materials. In addition, these initial results, indicate a promising way for start conciliating the Mott and Slater pictures in the physics of the strongly correlated electron systems.

PACS numbers: 71.10.Fd,71.15.Mb,71.27.+a,71.30.+h,74.20.-z,74.25.Ha, 74.25.Jb,74.72.-h

I. INTRODUCTION

The Hubbard type of models in the theory of strongly correlated electron systems are notably successful^{1,2,3,4,5,6,7,8,9,10,11,12,13,14,15,16,17,18,19,20}. In particular, it is remarkable the way they reproduce the properties of Mott insulators, such as metal-transitions oxides and copper-oxygen layered HTc compounds¹¹. However, the efforts for developing approaches having more basic foundations had not ceased, due to the expectation that they could open the way for obtaining more exact and specific results^{8,9,21}. In this sense, methods that are grouped into the so called Band Theory picture are also known as first principle calculations in the literature. They are electronic structure calculations that begin with the interactions among electrons or atoms in vacuum. The study of the band structure they predict, in principle should offer a road toward the effective and precise determination of the physical properties of each material^{21,22}. Some of them are: the Configurations Interaction scheme (CI); the Local Density Approximations method (LDA)²³, the Local Spin Density Approximations procedure (LSDA) and Hartree-Fock method (HF). However, the above mentioned potentialities of those first principles approaches had been failing in describing many of so called strongly correlated electron system¹¹. For example, the LSDA, a sophisticated generalization of the LDA procedure, was devised to describe local spin structures²¹. However, although the method had offered satisfactory descriptions of the physical results in few materials, this success had not been universal and it also wrongly predicted the properties of some compounds, by example, the here considered La_2CuO_4 .

The motivation of the present work arose from a primary suspicion that perhaps the self-consistent Hartree Fock (HF) method, could had been underestimated in its possibilities for helping in the above described searches^{2,24,25}. In this sense, it can be firstly remarked that it is widespread the criteria that for obtaining behaviors such as the Mott insulator character, it becomes necessary the presence of short range correlations among electrons with spin quantized in different directions. By example, paraphrasing one type of Mott's argument for specific systems:"... two electrons with spin resting on contrary directions are forbidden to occupy the same Wannier orbital... ". On another hand, the

orthodox HF approaches does not have in consideration the correlations among electrons of different spins. Therefore two electrons with opposite spins do not disturb one each other and consequently both of them can occupy the same Wannier orbital. Clearly, the usual HF approach, seems not to be viable for investigating a system in which the Mott's argument is appropriate. However, the physical sources of the validity of cited Mott's statement in some systems are not completely clear. By example: which is the physical origin of these short range correlations assumed in it?. Even, the proper concept of correlations, roughly described as: "everything missing in the single-particle HF state for to be the real many body ground state", makes clear how clouded their origins are. As the result of the study presented here, we believe that many of the so called correlation effects, can be effectively described even in the framework of the HF scheme, after removing certain symmetry restrictions which obstacle the finding of the best HF solutions. Such constraints are usually imposed on the space formed by the single particle orbitals, which are employed to construct the determinant like states among which the HF one shows minimal energy. By example, if after solving the HF problem, it occurs that the resulting self-consistent potential breaks the symmetry of the original crystalline lattice, it could create a gap and thus produce a Mott kind of insulating solution. This effect was originally discovered by Slater in Ref. 2. This symmetry breaking effect has been also more recently underlined and deepened in Ref. 27. However, the removal of this kind of symmetry restrictions alone had not been able to describe the insulator properties of a large class of materials^{11,21}. One of the central results of the present investigation, as it will be described just in what follows, is the identification of another important kind of symmetry restrictions that seemingly had been overlooked for long time. It can be cited here that a fully unrestricted formulation of the HF problem was early done by Dirac in Ref. 24.

This work will consider the Hartree-Fock self-consistent problem as applied to a simple one band model of the La_2CuO_4 ²⁶, but following an unusual way. In order to leave freedom to obtain paramagnetic, ferromagnetic and antiferromagnetic solutions in the same context, we look for single particle orbitals being non separable in their spacial and spinor dependence, i.e. they will have the structure $\phi(x, s) \neq \phi(x)\psi(s)$. In other words, in those states there is no an absolute common quantization direction for the electron spin. Thus, in each position the spin is quantized in a specific direction, and the equations of motion to be used will reflect this fact. Note, that to proceed in this way is not other thing that to apply the Dirac's unrestricted formulation of the HF procedure²⁴. We think that the restriction to α and β types of orbitals, usually employed in HF electronic band and quantum chemistry calculations, prohibits from the start the prediction of possible spontaneously symmetry breaking effects^{25,28}. Such a particular structure, excessively reduces the space of functions to be examined and consequently annihilates some possibilities to obtain exotic solutions (like that ones that are present in the strong correlation effects). We believe that in the context of the band theory, or more precisely, under the HF approach, it could be possible to reproduce the main characteristics of a wide class of *Mott insulator* kind of materials. The results of the simple model investigated here, as it will be seen, support this possibility for important compounds such as La_2CuO_4 , which under certain doping levels turn out in high temperature superconductors²⁶. The present work heads in that direction, with eyes in also showing the potentialities of implementing the above considerations in self-consistent HF calculations, not only for describing electronic bands and the associated ground states, but also for studying atomic and molecular structures.

The exposition proceeds as follows. In the Section II we describe the details of the HF self-consistent method to be employed in next sections. Specifically, it will be discussed the imposition of restrictions on the space of single particle states in which the solutions will be searched and the possible physical consequences they could carry on. In Section III the effective model we are going to employ will be exposed. The symmetry restrictions to be assumed and its corresponding tight-binding Bloch basis will be defined. Section IV is devoted to derive the HF equations associated to interacting electrons which free hamiltonian is given by the specially constructed effective tight binding model. The tight binding Bloch basis associated to the model is chosen in this section to have the maximal symmetry given by the group of translations leaving invariant the copper-oxygen plane in La_2CuO_4 . Considering the previously mentioned paramagnetic solution in a generic form, the free parameters of the effective hamiltonian are adjusted to reproduce the form of the only half filled band in the Matheiss calculation of the band structure of La_2CuO_4 ²². After defined the free hamiltonian of the model, the paramagnetic and antiferromagnetic solutions are obtained. The Bloch basis shown in Section III was employed. Both solutions are also compared in this section and the properties of all the obtained states are analyzed in corresponding subsections. Appendix A presents notations, algebraic developments, constants and definitions cited along the writing. In a final secci3n the main conclusions of the work are reviewed and various further tasks for its extension are described.

II. ROTATIONAL INVARIANT HARTREE-FOCK METHOD.

In the language of Quantum Mechanic the state of a system of N particles is described by a function depending on each one particle's spinor and spacial coordinates $f_n(x_1; s_1, \dots, x_N; s_N)$, where n represents the corresponding set of

quantum numbers²⁹. The HF approximation consists on supposing that the above mentioned state can be expressed as a linear combination of N -products of orthonormalized orbitals $\phi_{k_i}(x_i, s_i)$ with $i = 1, \dots, N$. Each one of these orbitals is interpreted as a single particle state, because it defines amplitude and probability distributions depending on a single particle coordinates. As usual, in what follows the word coordinates will mean the spacial as well as the spinor ones. If the particles are fermions, the previously mentioned linear combination is called Slater determinant^{25,28,29}.

Let

$$\hat{\mathcal{H}}(x_1, \dots, x_N) = \sum_i \hat{\mathcal{H}}_0(x_i) + \frac{1}{2} \sum_{j \neq i} V(x_i, x_j), \quad (1)$$

be the N -electrons system hamiltonian, including kinetic plus interaction with the environment hamiltonian $\hat{\mathcal{H}}_0$, besides Coulomb interaction among pairs of electrons V . The HF equations of motion for this system, leading the dynamic of the single particle states in a self-consistent way, are

$$\begin{aligned} & [\hat{\mathcal{H}}_0(x) + \sum_{\eta_1} \sum_{s'} \int d^2x' \phi_{\eta_1}^*(x', s') V(x, x') \phi_{\eta_1}(x', s')] \phi_{\eta}(x, s) \\ & - \sum_{\eta_1} [\sum_{s'} \int d^2x' \phi_{\eta_1}^*(x', s') V(x, x') \phi_{\eta}(x', s')] \phi_{\eta_1}(x, s) = \varepsilon_{\eta} \phi_{\eta}(x, s), \end{aligned} \quad (2)$$

where $\eta = k_1, \dots, k_N$ is a label in the basis formed by the solutions. That is, each HF electron state is influenced by the presence of the other ones. The self-consistent hamiltonian has two components, the coulomb like type of mean potential which their fellows create: the direct potential and the contribution reflecting the fact that two electrons cannot occupy the same state: the exchange potential²⁴.

The HF energy of the N electrons system and the interaction energy of an electron in the η state with the remaining ones, are given by

$$E_{HF} = \sum_{\eta} \langle \eta | \hat{\mathcal{H}}_0 | \eta \rangle + \frac{1}{2} \sum_{\eta, \eta_1} \langle \eta, \eta_1 | V | \eta_1, \eta \rangle - \frac{1}{2} \sum_{\eta, \eta_1} \langle \eta, \eta_1 | V | \eta, \eta_1 \rangle, \quad (3)$$

$$a_{\eta} = \frac{1}{2} \sum_{\eta_1} \langle \eta, \eta_1 | V | \eta_1, \eta \rangle - \frac{1}{2} \sum_{\eta_1} \langle \eta, \eta_1 | V | \eta, \eta_1 \rangle, \quad (4)$$

The bracket notation definition is given in Appendix A within the Subsection A 1. It can be noted that the system of equations (2) is rotational invariant because it is written without imposing a spatially absolute direction for the spin quantization of the single electron orbitals. This rotational invariant formulation of the self-consistent HF procedure was firstly introduced by Dirac in Ref. 24.

A. α, β and symmetry restrictions.

To solve (2) is a complicated task because it is a system of coupled integro-differential equations. The iterative method is one of the most frequently employed for solving this kind of systems and it is usually complemented by the imposition of symmetry restrictions that simplify the space of states to be investigated. However, the use of such constraints could avoid the obtaining of special solutions non obeying the added symmetry conditions. Although in some cases they could retain the minimal energy one, the method can hide the existence of interesting excited states and inclusive could wrongly predict the excitation features in some cases, as it will be seen in what follows. A very common symmetry restriction usually employed in band theory and quantum chemistry calculations is to consider that single particle solutions of (2) have spin quantized in a given direction in every point of the space^{22,28}. That is

$$\phi_{\mathbf{k}}(x, s) = \begin{cases} \phi_{\mathbf{k}}^{\alpha}(x) u_{\uparrow}(s) & \alpha \text{ state,} \\ \phi_{\mathbf{k}}^{\beta}(x) u_{\downarrow}(s) & \beta \text{ state,} \end{cases} \quad (5)$$

where $u_{\uparrow\downarrow}$ represent the Pauli spinors with spin up and down in a certain direction respectively. If the spacial functions $\phi_{\mathbf{k}}^{\alpha}$ and $\phi_{\mathbf{k}}^{\beta}$ are the same, the HF calculation is called a restricted one, if they are different, the procedure is called

unrestricted²⁸. It is interesting to investigate the consequences of considering the possibly existence of non separable single particle states being solutions of the HF problem. A positive answer to this question can open a natural context for obtaining solutions exhibiting magnetic properties and to allow their comparison with paramagnetic ones.

Another important kind of restrictions posed on the first principles band theory evaluations is the a priori impositions of crystal symmetries. To beforehand impose a symmetry on the assumed to be searched solution, although it could be well rooted in the studied system, has the risk of hiding a possible spontaneous breaking of that invariance. This could occurs due to the reduction of the space orbitals in which we are searching. In that case it can turns out that the obtained solutions will not be an absolute extremal of the energy functional, but a conditional one, due to the fixed symmetry constraint. For instance, let us consider the functional space formed by the allowed orbitals and the maximal subset of orbitals U which is invariant under a certain group of transformations \mathbf{T} . Consider also the maximal subset U_s being invariant under the group of transformations \mathbf{T}_s which is a subgroup of \mathbf{T} . Then, the set U_s obtained from imposing less symmetry restrictions a priori, should contain the set U . Therefore, after to find the extremes of the same functional in U and U_s , it could be possible to obtain different results. In this case, the solution in U_s , in general, shall be the most stable of both. However, also it could be the case that looking for a solution in U_s , an extremal function also pertaining to U arises as a solution. In such a situation, such a configuration could be found from the beginning by finding the extreme of the functional in U , that is, by imposing more symmetry restrictions. In terms of the HF scheme, this could mean that the states corresponding to both solutions have identical occupied single-particle states, but they curiously might show different sets of excited ones. Therefore, depending on the particular features of the material, removing a priori imposed symmetry restrictions on the set of allowed orbitals of the HF procedure, can predict new properties for the excited single particle states of the system. Such one could be for instance the gap appearance. This effect can have physical relevance after noting that at finite temperatures the more stable state will be preferred by the system and then the state showing a gap should be expected to be selected at non zero temperature.

III. TIGHT BINDING ELECTRON MODEL: "REMOVING SYMMETRIES".

In this section the basis of the effective band model used to describe the dynamic of the less bounded La_2CuO_4 electrons will be presented. The main considerations for defining the model and the determination of its characteristic parameters are given. In Subsection III A the simplified electronic model for the copper-oxygen planes, as well the main definitions in its structure are introduced. Subsections III B and III C are devoted to define the symmetry transformation group defining the tight binding Bloch basis.

A. Model for the Cu-O planes.

It is known that at low temperature La_2CuO_4 is an antiferromagnetic-insulator²⁶. However, in evident contradiction with the experiments the Linear Augmented Plane Waves (LAPW) technics²² predicts a metal and paramagnetic zero temperature properties for this material. Nevertheless, such band calculation results show that the conduction electrons are strongly coupled to the Bravais lattice centers of the copper oxygen planes. Clearly this tight-binding behavior is determined by the interaction of the electrons with its surrounding effective environment. This defines the initial hypothesis of our model.

The less bounded electron in the La_2CuO_4 molecule is the Cu^{2+} 's not paired one. That is, at difference from O^{2-} ions, Cu ones do not have their last shell (3d) closed. Those copper 3d electrons fill the last band of La_2CuO_4 solid and in what follows they shall be referred as: the electron gas. It seems appropriate to consider those electrons as strongly linked to CuO_2 cells and moreover, given the above mentioned arguments, with special preference for the Cu centers⁵. Thus, our Bravais lattice is going to be the squared net coincident with the array of copper sites (see the figure 1). The presence of electrons pertaining to the various fully filled bands in the material plus the nuclear charges, plays a double role in the model. Firstly, it will act as an effective polarizable environment, which screens the field created by electron charges constituting the electron gas in the half filled band. Consequently, we will introduce a dielectric constant ϵ which will screen the Coulomb interaction. Secondly, as suggested by its spacial distribution and magnitude, the mean field created by the environment will be assumed to act as a periodic potential W_γ being responsible for tight-binding confining of the electron to the Cu centers.

It is also primordial in the model to take into consideration the interaction F_b among the electron gas and the "jellium" neutralizing its charges. This background will be modeled here as a gaussian distribution of positive charges

$$\rho_b(\mathbf{y}) = \frac{1}{\pi b^2} \exp\left(-\frac{\mathbf{y}^2}{b^2}\right), \quad (6)$$

surrounding each lattice point and with characteristic radius b .

In resume, the free hamiltonian of the model takes the form

$$\begin{aligned}\hat{\mathcal{H}}_0(\mathbf{x}) &= \sum_{i=1}^N \frac{\hat{\mathbf{p}}_i^2}{2m} + W_\gamma(\mathbf{x}) + F_b(\mathbf{x}), \\ W_\gamma(\mathbf{x}) &= W_\gamma(\mathbf{x} + \mathbf{R}), \\ F_b(\mathbf{x}) &= \frac{e^2}{4\pi\epsilon\epsilon_0} \sum_{\mathbf{R}} \int d^2y \frac{\rho_b(\mathbf{y} - \mathbf{R})}{|\mathbf{x} - \mathbf{y}|}, \quad b \ll p,\end{aligned}\tag{7}$$

where $\hat{\mathbf{p}}_i^2$ is the i -th electron's squared momentum operator; m is the electron mass; ϵ_0 is the vacuum permitivity and

$$\mathbf{R} = \begin{cases} n_{x_1}p \hat{\mathbf{e}}_{x_1} + n_{x_2}p \hat{\mathbf{e}}_{x_2}, \\ \text{with } n_{x_1} \text{ and } n_{x_2} \in \mathbb{Z}, \end{cases}\tag{8}$$

moves on Bravais lattice. The versors $\hat{\mathbf{e}}_{x_1}$ and $\hat{\mathbf{e}}_{x_2}$ are resting on the direction defined by the lattice's nearest neighbours, see figure 1 a). It is known that the distance between Cu nearest neighbours is $p \approx 3.8 \text{ \AA}^{26}$. We also consider the interaction among pairs of electrons in the form

$$V(\mathbf{x}, \mathbf{y}) = \frac{e^2}{4\pi\epsilon\epsilon_0} \frac{1}{|\mathbf{x} - \mathbf{y}|},\tag{9}$$

which, as remarked above, includes a dielectric constant associated to the presence of the effective environment.

We are seeking here for HF solutions with orbitals having a non separable spin and orbit structures. Thus, it was considered that the spin can show a different projection for the different Wannier wavepackets to be superposed in defining those orbitals. The spin for each of them will be either α or β type, according they are linked either to one or the other of the two sublattices shown in figure 1 a). Thus, the single particle eigenstates will be chosen to be invariant, only under the reduced group of translations which transform each of those sublattices on itself.

It is important employ a procedure leaving independently identified the characteristics of the electron states in each one of the sublattices. That will allow to analyze solutions with dissimilar qualities in a same framework, that is: antiferromagnetic **AFM**, paramagnetic **PM** and ferromagnetic **FM** ones. For this purpose, let us define the points of the two sublattices with indices $r = 1, 2$, as follows

$$\begin{aligned}\mathbf{R}^{(r)} &= \sqrt{2}n_1p \hat{\mathbf{q}}_1 + \sqrt{2}n_2p \hat{\mathbf{q}}_2 + \mathbf{q}^{(r)} \\ &\text{with } n_1 \text{ and } n_2 \in \mathbb{Z}, \\ \mathbf{q}^{(r)} &= \begin{cases} \mathbf{0}, & \text{if } r=1, \\ p \hat{\mathbf{e}}_{x_1}, & \text{if } r=2, \end{cases}\end{aligned}\tag{10}$$

where $\hat{\mathbf{q}}_1$ and $\hat{\mathbf{q}}_2$ form the basis versors on each one of them.

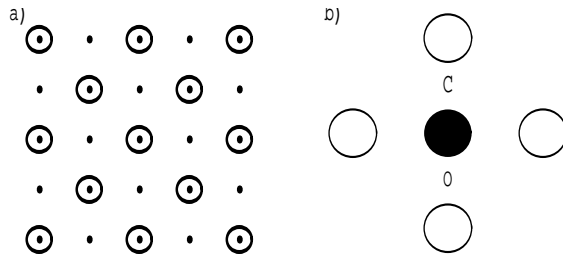


FIG. 1: The figures show: a) The point lattice associated to the Cu-O planes. For the search of the **AFM** properties of the conduction electron, and more generally for removing the symmetry restrictions, it will be helpful to separate the lattice in the two represented sublattices; and b) shows the corresponding base of the Cu-O planes.

B. Translations on the sublattices.

The solutions we are looking for will be eigenfunctions of the operators $\hat{T}_{\mathbf{R}^{(r)}}$ belonging to the reduced discrete translation group which transforms a given sublattice on itself:

$$\hat{T}_{\mathbf{R}^{(r)}} \phi_{\mathbf{k},l} = \exp(i \mathbf{k} \cdot \mathbf{R}^{(r)}) \phi_{\mathbf{k},l}. \quad (11)$$

If the Bravais lattice were infinite, the Brillouin's zone (B.Z.) associated to $\hat{T}_{\mathbf{R}^{(r)}}$ would be the shadowed one on figure 2 a). Note, that the continent square in this figure represents the B.Z. associated to the group of translations which leaves invariant the absolute lattice (the lattice formed by the Cu atoms in the CuO planes). However, given the impossibility of considering an infinite lattice for numerically solving the HF problem, then is also not allowed to consider its associated B.Z. as continuous. Therefore we will impose periodic boundary conditions on the $\phi_{\mathbf{k},l}$ in the absolute lattice's boundaries $x_1 = -L/p$ y L/p , $x_2 = -L/p$ y L/p (see figure 2 b)). This condition determines the allowed set of \mathbf{k}

$$\mathbf{k} = \begin{cases} \frac{2\pi}{Lp} (n_1 \hat{\mathbf{e}}_{x_1} + n_2 \hat{\mathbf{e}}_{x_2}), \\ \text{with } n_1, n_2 \in \mathbb{Z} \\ \text{and } -\frac{L}{2} \leq n_1 \pm n_2 < \frac{L}{2}. \end{cases} \quad (12)$$

Therefore, after recalling the discussion given in the introduction, note that we are now demanding less crystal symmetry on the single particle states which we are looking for, since a lower number of constraints are being imposed on the space of single particle states in which the solutions are searched.

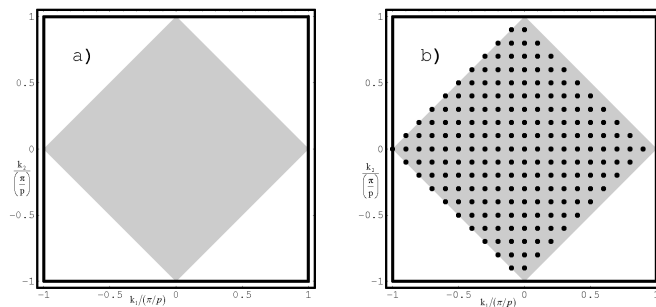


FIG. 2: In the figures: a) The Brillouin zone associated to the infinite absolute point lattice. The vectors \mathbf{k} label the eigenfunctions of the group of translations $\hat{T}_{\mathbf{R}^{(r)}}$ in this infinite point lattice. The grey square indicates the corresponding Brillouin zone (B.Z.) of the sublattices. The length of its side is $\sqrt{2}\pi/p$. b) The net of points shows the discrete character of the Brillouin zone when the absolute point lattice is finite with periodic conditions fixed in its boundaries. The unit of the scale means $\frac{\pi}{p}$.

C. Tight-Binding basis

The tight binding Bloch basis which we are going to use is the following

$$\begin{aligned} \varphi_{\mathbf{k}}^{(r,\sigma_z)}(\mathbf{x}, s) &= \sqrt{\frac{2}{N}} u^{\sigma_z}(s) \sum_{\mathbf{R}^{(r)}} \exp(i \mathbf{k} \cdot \mathbf{R}^{(r)}) \varphi_{\mathbf{R}^{(r)}}(\mathbf{x}), \\ \hat{\sigma}_z u^{\sigma_z} &= \sigma_z u^{\sigma_z}, \\ \varphi_{\mathbf{R}^{(r)}}(\mathbf{x}) &= \frac{1}{\sqrt{\pi a^2}} \exp\left(-\frac{(\mathbf{x} - \mathbf{R}^{(r)})^2}{2 a^2}\right), \quad a \ll p, \end{aligned} \quad (13)$$

where N is the number of electrons in the electron gas, $\hat{\sigma}_z$ is the spin z projection operator, where z is the orthogonal direction to the copper oxygen CuO_2 planes; $\sigma_z = -1, 1$, are the eigenvalue of the previously mentioned operator and $r = 1, 2$, is the label which indicates each one of the sublattices. As we are going to work on a half filling condition,

then N coincides with the number of cells in the crystal with fixed periodic boundary conditions N_c . Note, that due to the tiny overlapping among nearest neighbors approximation, the exact orthogonal character is only weakly lost between elements corresponding to different sublattices and having the same spin quantization. That occurs because nearest neighbors belong to different arrays. However the orthogonality between different elements corresponding to the same sublattice, as well as unity norm for every elements, is rigourously maintained. This follows because they are constructed as Bloch states in their corresponding sublattices. The Wannier orbitals $\varphi_0(\mathbf{x} - \mathbf{R}^{(r)})$ represent the probability amplitude of encountering one electron in the vicinity of the site $\mathbf{R}^{(r)}$, that is on the given cell CuO_2 .

Let us now describe some simplifications that will be adopted in order to solve the HF problem. The central aim of this work is not to make an exact study of the problem, instead we seek for approximate solutions qualitatively well reflecting the physical properties of La_2CuO_4 and other compounds. Following this principle we take for the Wannier orbitals the explicit form given in (13). Physically, this means to consider the effective potential created by the environment on each electron of the half filled band, is a quadratic function having a minimum on the copper sites and strongly confining the electrons to it. This last consideration is similar to the one made on the t - J one band model.

IV. MATRIX PROBLEM AND SOLUTIONS.

In this section the main results of this work and their discussion are presented. In Subsection IV A the equivalent matrix problem, resulting from projecting the HF system of equations (2) on the tight binding Bloch basis (13) defined in the previous section is presented. Subsection IV B shows how after imposing the maximal translational symmetry and an α and β spin nature on the orbitals, the model is able to reproduce the dispersion relation of La_2CuO_4 metal-paramagnetic half filled band of the precise band calculations given in Ref. 22. The solutions presented in subsections IV C and IV D, illustrate the consequences of releasing symmetry restrictions on the space in which HF solutions are searched. The first of them corresponds to a Mott's insulator-antiferromagnetic ground state. That is, the state corresponds to an insulator even though it has one electron per cell, precisely in the same way as La_2CuO_4 behaves. The second solution obtained corresponds to a paramagnetic state showing a pseudogap and exactly the same HF energy and set of occupied single particle states, that the previously obtained metal-paramagnetic state²². It is important to mention that all the band diagrams shown in this section are plotted on the same energy scale and the zero energy point coincides with the Fermi level of the antiferromagnetic ground state (IAF) presented in Subsection IV C.

A. Tight-Binding representation.

Let the searched single particle states represented in the explicitly nonseparable form

$$\phi_{\mathbf{k}, l}(\mathbf{x}, s) = \sum_{r, \sigma_z} B_{r, \sigma_z}^{\mathbf{k}, l} \varphi_{\mathbf{k}}^{(r, \sigma_z)}(\mathbf{x}, s), \quad (14)$$

where l is the additional quantum number needed for indexing the stationary state on question, which we are going to define precisely further ahead. After substituting (14), (7) and (9), in (2); followed by projecting the obtained result on the basis $\varphi_{\mathbf{k}'}^{(t, \alpha_z)}$ and an extensive algebraic work, it is possible to arrive at the following self-consistent matrix problem for the coefficients appearing in the expansion (14):

$$[\mathbf{E}_{\mathbf{k}}^0 + \tilde{\chi} (\mathbf{G}_{\mathbf{k}}^{dir} - \mathbf{G}_{\mathbf{k}}^{ind} - \mathbf{F}_{\mathbf{k}})] \cdot \mathbf{B}^{\mathbf{k}, l} = \tilde{\varepsilon}_l(\mathbf{k}) \mathbf{I}_{\mathbf{k}} \cdot \mathbf{B}^{\mathbf{k}, l}, \quad (15)$$

where each of the quantities

$$\mathbf{B}^{\mathbf{k}, l} = \|B_{(r, \sigma_z)}^{\mathbf{k}, l}\|, \quad (16)$$

represents a vector having four components given by the four possible pairs (r, σ_z) . The constants

$$\begin{aligned} \tilde{\chi} &\equiv \frac{me^2}{4\pi\hbar^2\epsilon\epsilon_0} \frac{a^2}{p}, \\ \tilde{\varepsilon}_l(\mathbf{k}) &\equiv \frac{ma^2}{\hbar^2} \varepsilon_l(\mathbf{k}), \end{aligned} \quad (17)$$

are dimensionless. In them, e represents the vacuum charge of the electron; \hbar is the reduced Planck constant; a is the characteristic radius of the Wannier orbitals φ_0 and p is the nearest neighbors separation. It is clear now that we can define $l = 1, 2, 3, 4$, as a label indicating each of the four solutions to be obtained for every value of quasi-momentum \mathbf{k} . Also, all the implicit parameters in the following 4×4 matrices are dimensionless

$$\begin{aligned} E_{\mathbf{k}}^0 &= \|E_{\mathbf{k},(t,\alpha_z);(r,\sigma_z)}^0\|, \\ G_{\mathbf{k}}^{dir} &= \|G_{\mathbf{k},(t,\alpha_z);(r,\sigma_z)}^{dir}\|, \\ G_{\mathbf{k}}^{ind} &= \|G_{\mathbf{k},(t,\alpha_z);(r,\sigma_z)}^{ind}\|, \\ F_{\mathbf{k}} &= \|F_{\mathbf{k},(t,\alpha_z);(r,\sigma_z)}\|, \\ I_{\mathbf{k}} &= \|I_{\mathbf{k},(t,\alpha_z);(r,\sigma_z)}\|. \end{aligned} \quad (18)$$

The set of quantities (18) constitute the matrix representations of the periodic potential created by the mean field W_γ , the direct and exchange terms in (2), the interaction potential with the neutralizing "jellium" of charges F_b defined in (7) and the overlapping matrix among nearest neighbors, respectively. Each one of the four pairs, (t, α_z) and (r, σ_z) defines a row and a column respectively, of the matrix in question. The explicit forms of the matrix elements are given in Appendix A.

In this new representation the normalization condition for the HF single particle states and the HF energy of the system take the forms

$$1 = \mathbf{B}^{\mathbf{k},l*} \cdot \mathbf{I}_{\mathbf{k}} \cdot \mathbf{B}^{\mathbf{k},l}, \quad (19)$$

$$E_{\mathbf{k},l}^{HF} = \sum_{\mathbf{k},l} \Theta(\tilde{\varepsilon}_F - \tilde{\varepsilon}_l(\mathbf{k})) [\tilde{\varepsilon}_l(\mathbf{k}) - \frac{\tilde{\chi}}{2} \mathbf{B}^{\mathbf{k},l*} \cdot (\mathbf{G}_{\mathbf{k}}^{dir} - \mathbf{G}_{\mathbf{k}}^{ind}) \cdot \mathbf{B}^{\mathbf{k},l}], \quad (20)$$

where Θ is the Heaviside function.

The system (15) is non linear on the variables $B_{r,\sigma_z}^{\mathbf{k},l}$, which are the four components of each vector $\mathbf{B}^{\mathbf{k},l}$. They can be interpreted as a measure of the probability amplitude of finding an electron in the state (\mathbf{k}, l) , in the sublattice r , with spin z-projection σ_z . Thinking in numerically solving the equations by the method of iterations, it is convenient to pre-multiply them by $\mathbf{I}_{\mathbf{k}}$ for each \mathbf{k} . Note that for each \mathbf{k} four eigenvalues ($l = 1, 2, 3, 4$) will be obtained, or equivalently, four bands on the Z.B. (Eq. 23). From Eq. (15) it can be observed that in the representation (13), the HF potentials and in general the total hamiltonian of the system, resulted as block diagonal with respect the sets of states indexed by the same \mathbf{k} . This fact is a consequence of the commutation of each one of them with every element of the reduced group of discrete translations. That is, the group of translations which leaves invariant a sublattice.

B. Maximally translational symmetric solutions.

In this subsection we will search for HF solutions having their orbitals on the space of Bloch functions being eigenfunction of the maximal group of translations leaving invariant the absolute lattice. In other words, we demand the maximum possible symmetry under translations. It will follows that our model is capable of acceptably reproduce the profile of the conduction band dispersion calculated in Ref. 22 for the La_2CuO_4 . We will adjust the free parameters of the model in order to reproduce in the best way the band dispersion reported in Ref. 22. The parameters are: the dielectric constant of the effective environment ϵ ; the characteristic radius of the gaussian Wannier orbitals \tilde{a} ; the jumping probability between nearest sites for an electron $\tilde{\gamma}$ (it is fixed by the effective environment) and the radius in which the gaussian orbitals associated to the neutralizing "jellium" of charges decays \tilde{b} (see Section III A).

In what follows the wavy hats will mean dimensionless, see Appendix A(A2). Let us define the Bloch basis for the space of orbitals in which the solution will be searched as

$$\tilde{\varphi}_{\mathbf{Q}}^{\sigma_z}(\mathbf{x}, s) = \sqrt{\frac{1}{N}} u^{\sigma_z}(s) \sum_{\mathbf{R}} \varphi_0^{\mathbf{Q}}(\mathbf{x} - \mathbf{R}) \quad (21)$$

$$\varphi_0^{\mathbf{Q}}(\mathbf{x}) = \exp(i \mathbf{Q} \cdot \mathbf{R}) \varphi_0(\mathbf{x}), \quad (22)$$

where

$$\mathbf{Q} = \begin{cases} \frac{2\pi}{Lp} (n_{x_1} \hat{e}_{x_1} + n_{x_2} \hat{e}_{x_2}), \\ \text{with } n_{x_1}, n_{x_2} \in \mathbb{Z}, \\ \text{and } -\frac{L}{2} \leq n_{x_1}, n_{x_2} < \frac{L}{2}. \end{cases} \quad (23)$$

are the quasimomenta of the single particle Bloch states which are eigenfunctions of the maximal group of translations. Also is important to define $N = L \times L$, and \mathbf{R} , which are the amount of cells in the absolute lattice and the corresponding parametrization (8), respectively. The functions $\varphi_0(\mathbf{x})$ are the gaussian orbitals defined in Section III C. The searched HF orbitals will have the form

$$\bar{\phi}_{\mathbf{Q},l}(\mathbf{x},s) = \sum_{\sigma_z} \bar{B}_{\sigma_z}^{\mathbf{Q},l} \bar{\varphi}_{\mathbf{Q}}^{\sigma_z}(\mathbf{x},s), \quad (24)$$

as expressed on the above mentioned basis. This time, the equivalent matrix problem for the "vector" $\bar{B}^{\mathbf{Q},l}$ is of second order for each value of (\mathbf{Q},l) . That is, its solutions will be two component vectors. Consequently, l will take the values 1 or 2 now. Thus, in analogy to (15) the new set of equations to be solved results in the form

$$[\bar{E}_{\mathbf{Q}}^0 + \tilde{\chi} (\bar{G}_{\mathbf{Q}}^{dir} - \bar{G}_{\mathbf{Q}}^{ind} - \bar{F}_{\mathbf{Q}})] \cdot \bar{B}^{\mathbf{Q},l} = \tilde{\varepsilon}_l(\mathbf{Q}) \bar{I}_{\mathbf{Q}} \cdot \bar{B}^{\mathbf{Q},l}. \quad (25)$$

Let $\bar{\Upsilon}$ and Υ any one of the 2x2 matrices in (25) and its 4x4 equivalent on (15) respectively, the relationship between these matrix elements is the following one

$$\bar{\Upsilon}_{(\alpha_z, \sigma_z)} = \frac{1}{2} \sum_{t,r} \Upsilon_{(t, \alpha_z); (r, \sigma_z)}. \quad (26)$$

The direct and exchange potentials respective matrices 2x2 and 4x4 relationship becomes slightly more complicated. Besides also satisfying the above mentioned relation, each vector components in their "4x4" definitions must be removed from the sublattice label dependence and multiplied by $\frac{1}{\sqrt{2}}$ (those new quantities are the vector components of the 2x2 problem). For instance, making reference to the definitions given in Appendix A

$$\bar{I}_{\mathbf{Q},(\alpha_z, \sigma_z)} = \delta_{\alpha_z, \sigma_z} [I_{00} + 2I_{01}(\cos Q_1 p + \cos Q_2 p)].$$

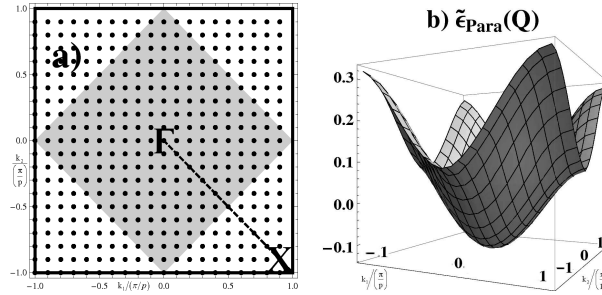


FIG. 3: The figure a) shows the Brillouin zone associated to the absolute point lattice. The grey zone signals the occupied states in the paramagnetic metallic solution at half filling conditions. The unity of quasimomentum is $\frac{\pi}{p}$. Figure b) shows the doubly degenerated bands associated to the same paramagnetic and metallic state. Note the close correspondence between these results and the ones obtained by Matheiss in Ref. 22. The zero energy level in all the band diagrams is the Fermi energy of the isolator and antiferromagnetic solution presented in subsection IV C. The domain of the plot is the B.Z. of the sublattice shown in Fig. 2 a).

Analogously to the ones showed in the previous section, in this representation, the normalization condition for the single particle states and the HF energy of the system take the forms

$$1 = \bar{B}^{\mathbf{Q},l*} \cdot \bar{I}_{\mathbf{Q}} \cdot \bar{B}^{\mathbf{Q},l}, \quad (27)$$

$$\bar{E}_{\mathbf{Q},l}^{HF} = \sum_{\mathbf{Q},l} \Theta_{(\tilde{\varepsilon}_F - \tilde{\varepsilon}_l(\mathbf{Q}))} [\tilde{\varepsilon}_l(\mathbf{Q}) - \frac{\tilde{\chi}}{2} \bar{B}^{\mathbf{Q},l*} \cdot (\bar{G}_{\mathbf{Q}}^{dir} - \bar{G}_{\mathbf{Q}}^{ind}) \cdot \bar{B}^{\mathbf{Q},l}]. \quad (28)$$

The method employed for solving all the self-consistent matrix problems considered in this work was an iterative one which started from a particular and estimated as convenient state configuration. In the case being examined in this section, for beginning the iterations, we used a paramagnetic state. The figure 3 shows the paramagnetic, metallic and doubly degenerate band obtained from the iterative process on (25). A half filling condition has been assumed, that is, a state with one electron per cell is being considered. Specifically, for the case of $N = 20 \times 20$ electrons,

the occupied states inside the B.Z. are showed in figure 3 a) by the points inside the shadowed region. The chosen parameters were: $\epsilon=10$, which is a common value for semiconductors, $\tilde{a}=0.25$, $\tilde{b}=0.05$ and $\tilde{\gamma}=-0.03$ (see Appendix A), by following the criterium of fixing a bandwidth of 3.8 eV²². The here obtained band topologically coincides with the conduction band presented in Ref. 22. In both of them the Fermi level on the Γ - X direction is a square which vertices touch the middle of the B.Z. (of the CuO lattices) sides and also the maximal and minimal energies lay on coinciding points. Therefore, in this subsection the basis of the effective model employed here and its main set of parameters have been defined.

C. Insulating and antiferromagnetic solutions.

As we have stated before, the solution of the system of equations Eq. (15) was performed by the method of successive iterations. The results which presented from now on were found by employing the parameter values ϵ , \tilde{a} , $\tilde{\gamma}$ and \tilde{b} , which were determined in the previous section. It is important to be noted that \tilde{a} , $\tilde{b} \ll 1$ and also that $\tilde{\gamma}$ must be of the order of the overlapping among nearest neighbors factor. It was necessary to start the iteration process from a particular state having an antiferromagnetic character from the beginning, in order to achieve convergence toward the solution presented in this subsection. In the figure 4 two sets of results following for a half filling band are shown. They correspond to two lattices of 20x20 and 30x30 cells. The bands are depicted on the same scale of energies. The difference between them is of the order of 10^{-5} dimensionless units of energy $\frac{\hbar^2}{ma^2} = 8.3$ eV. Evidently, they are bands corresponding to insulating states. The close similarity of both results indicates that the thermodynamical limit has being satisfactorily achieved for the considered sizes of the periodic system. The HF energy of this HF solution was the lowest among of all the ones found. In coincidence with the experimental evidence, they are states with local magnetic moment resting on the direction of the sublattice x_{12} (see figure 5). In the next section we will show the difference between this HF energy of this state and the ones corresponding to the other determined HF solutions and shall comment on this respect.

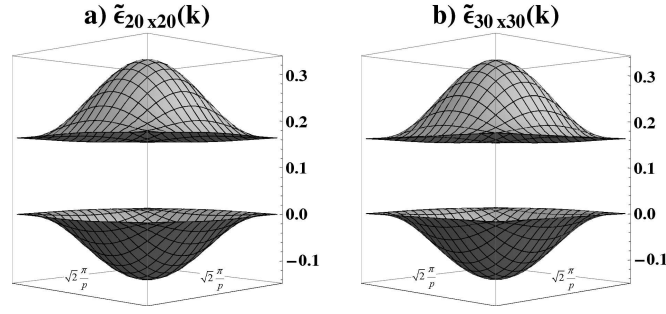


FIG. 4: Energy bands obtained for: a) A sample of 20x20 cells, $E_{gap} = 1.32$ eV. b) A sample of 30x30 cells, $E_{gap} = 1.32$ eV. The parameter values chosen were $\tilde{a} = 0.25$, $\tilde{b} = 0.05$, $\tilde{\gamma} = -0.03$ and $\epsilon = 10$. The zero energy level is fixed in the Fermi level of the 20x20 system. Note that the difference in energy between the two bands is not appreciable in the employed energy scale. The domains of both plots is the B.Z. of the sublattice shown in Fig. 2 a)

One important quantity which has been experimentally measured is the magnetization. It is therefore motivating to inspect the prediction of the obtained HF state for this magnitude. Its definition is given by the expression

$$\mathbf{m}(\mathbf{x}) = \sum_{\mathbf{k}',1} \sum_{s,s'} \phi_{\mathbf{k}',1}^*(\mathbf{x}, s) \boldsymbol{\sigma}(s, s') \phi_{\mathbf{k}',1}(\mathbf{x}, s'), \quad (29)$$

where

$$\boldsymbol{\sigma}(s, s') = \sigma_{x_1}(s, s') \hat{\mathbf{e}}_{x_1} + \sigma_{x_2}(s, s') \hat{\mathbf{e}}_{x_2} + \sigma_z(s, s') \hat{\mathbf{e}}_z,$$

and $\sigma_{x_1} = \begin{pmatrix} 0 & 1 \\ 1 & 0 \end{pmatrix}$, $\sigma_{x_2} = \begin{pmatrix} 0 & i \\ -i & 0 \end{pmatrix}$ and $\sigma_z = \begin{pmatrix} 1 & 0 \\ 0 & -1 \end{pmatrix}$ are the Pauli matrices.

In figure 5 a) the only non vanishing component of (29) in this solution is plotted. An interesting result is that it has been experimentally observed that La_2CuO_4 has a magnetic moment of $0.68 \mu_B$ per Cu site on the CuO plane²⁶. The value obtained from evaluating the above formula for our HF state turns out to be $0.67 \mu_B$. Therefore, the considered here discussion satisfactorily predicts the whole antiferromagnetic structure of La_2CuO_4 .

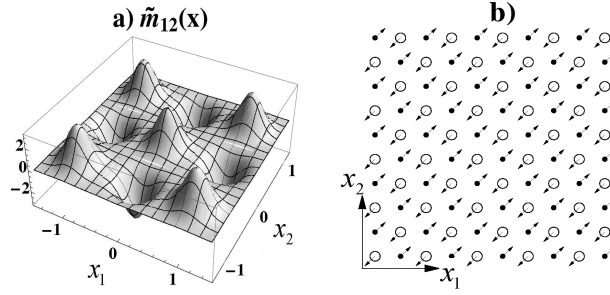


FIG. 5: The magnetizaion vector \mathbf{m} of the more stable HF state here determined rests in the direction 1-2. a) This figure shows the projection \tilde{m}_{12} of the dimensionless magnetization, in the 1-2 direction. The magnetization unit is $\frac{\mu_B}{p^2}$. b) The picture shows a scheme of the mean magnetic moment per site in the lattice. For the shown solution its modular value is $0.67\mu_B$.

It is also helpful to remark that the corresponding single particle states carry a more intensive antiferromagnetism as more closer they are from the Fermi surface. Therefore, this property offers a clear explanation of the gradual loss observed in the antiferromagnetic order under the doping with holes¹¹. In figure 6 the dependence of the angle ϕ between the magnetic moments per cell on each of the sublattice 1 and 2, shown by each one of the single particle Bloch states, is plotted. These components are defined as the integrals of the magnetic moment density over all the unit cells of the *absolute* lattice centered in the sublattice points. Note that the states laying just on the Fermi surface are perfectly antiferromagnetic ones, and that the more away from the boundaries the orbitals are, the less antiferromagnetic they become. Then, this HF solution indicates that after the orbitals are allowed to spatial dependent spin orientations, the electrons prefer to reorient their spin when traveling between contiguous lattice cells. This effect that can be interpreted as clean "correlation" effect when considered within a restricted HF picture..

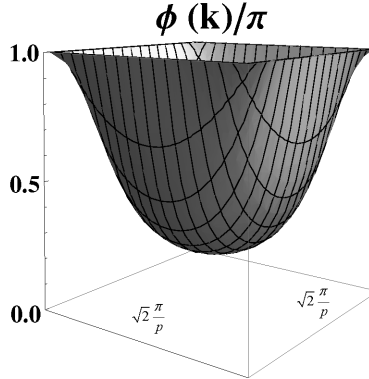


FIG. 6: The single particle states exhibit a sharp antiferromagnetism in the proximities of B.Z. boundaries. In the figure the angle between their magnetic moment components on each of both sublattices (after divided by π) is plotted against their Bloch states quasimomenta. Note that the states on the boundary have a perfect antiferromagnetism and that they become less antiferromagnetic as their quasimomenta move away from the boundary. The region of the plot is the B.Z. of the sublattice shown in Fig. 2 a)

It also follows that the size of the zone in which the antiferromagnetism is strongest, inversely depends on the dielectric constant. Thus, the less is the Coulomb interaction among the electrons in the half filled electron band, smaller becomes the antiferromagnetic character of the single particle states and the region in which the antiferromagnetism accumulate. Only the single particle states staying exactly on the Fermi surface remain having a perfect antiferromagnetism. In addition, the magnitude of the gap also decreases with the increasing of the dielectric constant.

D. Paramagnetic solution showing a pseudogap.

It can be observed that to remove the translational symmetry restrictions does not mean renouncing to obtain a paramagnetic state as solution. As a matter of fact, this solution effectively exists and its properties are quite

interesting. In Section I we had already commented about La_2CuO_4 and its antiferromagnetic *Mott's insulator* properties. However, at an intermediate level of doping, this material presents very special properties. After the breaking of the antiferromagnetic order and in a certain temperature T and doping ranges, the material transits to phases showing a so called pseudogap. In the La_2CuO_4 and other HTc materials the presence of this property has been observed in some regions of their paramagnetic phase **PM** and in the superconductor phase **SC**¹⁴.

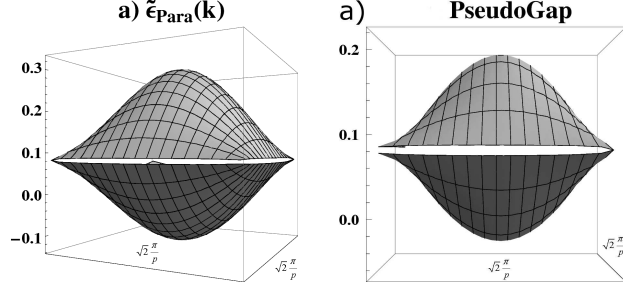


FIG. 7: In the figure: a) The band structure associated to paramagnetic ground state showing a pseudogap is shown. b) A frontal view of the plot more clearly showing the pseudogap. The zero energy level is the Fermi energy of the IAF solution. The two graphics are plotted in the B. Z. of the sublattices, that is, the grey zone in figure 2 a).

In figure 7 the band spectra corresponding to the HF paramagnetic ground state obtained from Eq. (15) is shown. Note the existence of a pseudogap which reaches a maximum value of $0.1 \text{ eV} \approx 10^3 \text{ K}$ (equivalent to 0.012 dimensionless unit of energy $\frac{\hbar^2}{ma^2} = 8.3 \text{ eV}$). The parameters given in the Subsection IV B were employed for this evaluation. The pseudogap amplitude rises for smaller dielectric constants ϵ , that is, with the reduction of the screening. It is an interesting result that the HF energy of this ground state is exactly coincident with the one corresponding to the paramagnetic and metallic state presented in Subsection IV B. Moreover, the lowest energy band in both solutions, also exactly coincide, with an upper bound error of 10^{-6} in dimensionless energy units (that means 10^{-5} in eV). Thus, the occupied single particle states in both solutions are identical and in consequence the momentum dependence of the filled energy bands also coincide. Henceforth, the difference between the two solutions refers only to the non occupied states. Those states can not be considered in the band model presented in Subsection IV B. For instance, consider the expressions for two states, one occupied and another empty, which are associated to the same four quasimomentum value

$$B_o^{\mathbf{K}} = \begin{pmatrix} \frac{1}{\sqrt{2}} \\ \frac{1}{\sqrt{2}} \\ 0 \\ 0 \end{pmatrix} \rightarrow \phi_o(\mathbf{x}, s) = \sqrt{\frac{1}{N}} u_{\uparrow}(s) \sum_{r, \mathbf{R}^{(r)}} \exp(i \mathbf{K} \cdot \mathbf{R}^{(r)}) \varphi_{\mathbf{R}^{(r)}}(\mathbf{x}), \quad (30)$$

$$B_e^{\mathbf{K}} = \begin{pmatrix} \frac{1}{\sqrt{2}} \\ -\frac{1}{\sqrt{2}} \\ 0 \\ 0 \end{pmatrix} \rightarrow \phi_e(\mathbf{x}, s) = \sqrt{\frac{1}{N}} u_{\uparrow}(s) \sum_{r, \mathbf{R}^{(r)}} (-1)^r \exp(i \mathbf{K} \cdot \mathbf{R}^{(r)}) \varphi_{\mathbf{R}^{(r)}}(\mathbf{x}), \quad (31)$$

where $\varphi_{\mathbf{R}^{(r)}}$ represents the gaussian orbitals φ_0 centered on $\mathbf{R}^{(r)}$.

Comparing with the expression (24), it may be noted that the occupied single particle state (30) can be expressed on the basis (21), and in fact, coincides with the state $\bar{\phi}_o^{\mathbf{K}, \uparrow}$ obtained from solving (25). However the excited state (31) was not allowed in the space of orbitals employed in solving (25), and thus its attainment is a neat consequence of the removing of the usually imposed symmetry under the maximal group of translations. More precisely, these excited states showing a pseudogap, appeared thanks to the allowed independence between the Bloch functions defined in both sublattices, introduced in this work. This result shows an interesting potential use that this kind of constraints removing procedure could introduce in the determination of new excitation properties of the HF solutions in various applications.

In the following table the HF energies per particle are shown for the paramagnetic-metallic (PM), paramagnetic with pseudogap (PPG) and insulator-antiferromagnetic (IAF) ground states; with zero point energy assumed on the last one:

It is an interesting outcome that the energy difference PM (PPG)-IAF and the Néel temperature of this kind of materials are both of the order of 10^2 K . Thus, the results suggest the possibility of having further success in applying

State	IAF	PM	PPG
ΔE (eV)	0.0	+0.076	+0.076

TABLE I: Energy differences between the various HF states.

the approach started in this work to the description of some regions of the phase diagram of the La_2CuO_4 . On the question about the relative stability between the PM and PPG states, it can be estimated that due to the presence of a pseudogap, the PPG ground state should become more stable than the PM at non vanishing temperatures. This should be the case because for creating excitations on the PPG ground state, temperatures of hundreds of Kelvin degrees are needed, while excitations in the PM ground state can occur in every range of temperatures.

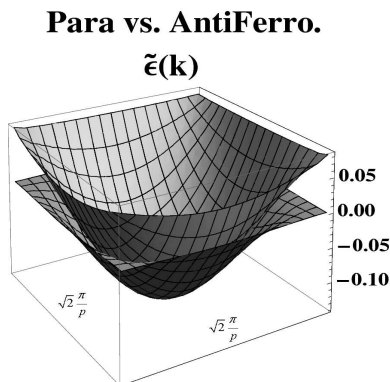


FIG. 8: The figure shows in the same plot the occupied bands corresponding to the states PPG and IAF. The difference in the energies of the orbitals is concentrated in the boundary of the Brillouin zone. The zero energy level coincides with the Fermi level of the IAF solution. The domain of the plot is the B.Z. of the sublattices, given by the grey zone in figure 2 a).

In figure 8 the PPG (PM) and IAF occupied bands are depicted in a common frame. The main difference in their energies corresponds to the single particle states being closer to Fermi surface. As we had noted before, the same behavior has the antiferromagnetic character of the single particle states of the IAF solution. Therefore, it can be hoped that from the solution of (25) under doping with holes, both solutions move toward a common ground state without absolute magnetic order, in correspondence with the pattern shown by the phase diagrams of these materials²⁶. That is, at a critical doping level value a breaking of the antiferromagnetic order could occur and the system presumably transits to a phase showing a pseudogap.

V. CONCLUSIONS

The results of this work support the potential of the HF self-consistent method for the description of some secular properties exhibited by materials such as copper-oxygen compounds, specifically La_2CuO_4 . Those are properties usually associated to strong correlation effects, that could be explained by *first principle* calculations, after modified to incorporate procedures to search for spontaneous symmetry breaking solutions and general ways of exploring the spin structure of the HF orbitals. Note that single particle orbitals are not only employed in the HF method. They are also essential ingredients of more general schemes as the various types of density functional methods. Thus, the kind of reasoning employed in this work seems to be easily easily implemented in such discussions. In the present work we explore those paths in a simplified manner. In order to avoid the intrinsic complexities of La_2CuO_4 material, it was necessary to utilize a simple model which was sufficiently flexible for reproducing the dispersion profile of the only half filled band of La_2CuO_4 reported in Ref. 22. After imposing the maximal symmetry under translations a paramagnetic and metallic ground state (PM) was obtained which dispersion properties topologically also coincide with the results given in Ref. 22. Then, the free parameters of effective model were fixed from the requirement of reproducing the bandwidth of the half filled band obtained in Ref. 22. Employing those parameters and from removing some symmetry restrictions, solutions were obtained which show interesting properties. In agreement with the experiment, the insulating-antiferromagnetic (IAF) solution turns to be the most stable among all HF states found. Some of its properties are enumerated below:

1. The gap magnitude diminish with the increasing of the screening constant ϵ .
2. The antiferromagnetic structure the HF orbitals increases when the states approach the Fermi level. In addition, the size of the outlying region in which antiferromagnetism persists depends on the screening created by the effective environment ϵ . That is, by increasing screening, the size of the antiferromagnetic region reduces. Thus, the idea arises that after doping with holes (that is, solving for HF solutions not at half filling condition as it is done here) the antiferromagnetic zone, which is precisely concentrated near the Fermi level could be annihilated, producing in this way a phase transition to a non magnetically ordered ground state. This possibility indicates a way to describe the normal state properties of the HTc superconductors through a simple HF study.
3. The magnetic moments per cell which are evaluated rest on the right direction respect to the lattice and its modular value of $0.67 \mu_B$ satisfactorily coincides with the experimentally measured result $0.68 \mu_B$. This outcome support the adjust made of the parameters defining the effective model employed.

The other HF solution presented in this work corresponds to a paramagnetic state showing a pseudogap (PPG). Few properties of this state are described in what follows:

1. The pseudogap magnitude diminishes with the increasing of the screening constant ϵ .
2. Just as we hoped from the beginning of the work, at zero temperature the states PM and PPG resulted identical. The difference between them is only given by the excitations of the system. Thus, the removal of some symmetry restrictions, defines in this case, new properties for unoccupied single particle states. It seems feasible that in other materials, it could be possible to obtain a gap instead of a pseudogap even in the absence of magnetic order. Such an outcome could show the ability of a properly formulated HF description in describing all the kinds of Mott insulators, being or not magnetically ordered.
3. The amplitude of the obtained pseudogap reaches a value of the order of 10^2K . Thus, it is possible that the system at finite temperature should prefer the PPG state over the PM one. That is an interesting signal, knowing that $\text{La}_{2-x}\text{M}_x\text{CuO}_4$ presents pseudogap in the **PM** phase.
4. In the same way as it happens for the antiferromagnetic character of the IAF ground state, the difference between the one particle energies of IAF and the PPG (PM) states, is greater for states being closer to the Fermi surface. That is, it happens for the electrons with more energy and consequently the first ones in disappear under doping with holes. Therefore, as it was mentioned before, these results suggest the possibility to describe a transition IAF \rightarrow PPG under doping with holes, within the here studied effective model.

One methodological conclusion of this work seems to be worth to be mention. It corresponds to the fact that the results fully clarifies that the solutions of a general HF problem non necessarily should turn to be a set of single particle orbitals, all having an α or β spin structure at all points of the space. This is directly shown by the particular example of the IAF solution in which the HF single particle states have a neatly non separable character in their spin and orbital dependence. This possibility, although being simple, and perhaps even expected to be correct after to direct the attention to it, looks to be relevant for the description of magnetic and strongly correlated systems.

The above enumerated conclusions motivated new objectives to be considered in extending the work. Our general interests are twofold: in one side to achieve a more complete and precise investigation about the here detected unexplored potentialities of the *first principle* calculations. In another direction, to look for the possibility of describing the HTc superconductivity in the framework of the here studied simple model. Some of the more specific issues of future searches in connection those general objectives are the following ones:

- To generalize the discussion done in this work to introduce the doping with holes as a new parameter. Then, it will be possible to investigate the effects of the doping on the here determined ground states. Of particular relevance in this sense appears the IAF state.
- To compute the zero temperature electron Green function of the system, and use it to evaluate the effective polarization of the La_2CuO_4 in the obtained states.
- With the polarization results at hand, attempt to solve the Bethe-Salpeter equation for two holes in the IAF ground state (and also in the PPG one), to find whether it is possible or not to define the existence of preformed Cooper Pairs in the model. The possibility for its existence was suggested by the results of Ref. 30, in which it was argued that a strong 2D-screening of the Coulomb interaction is created by a half filled band of tight binding electron.
- To continue the application of the ideas advanced here in help clarifying the widely known debate between the Mott and Slater pictures about the electronic structure of solids.

- To apply a rotational invariant HF calculation for obtaining states of molecular or atomic systems having incomplete shells. We guess, that this application could help to reduce the value of the correlation energies in those systems. This idea is suggested by the results of this work which show that the HF energy can be optimized in many of the currently considered physical systems, due to the difficulties in determining the best among all possible self-consistent solutions.

Acknowledgments

We express our gratitude to A. González, C. Rodríguez, A. Delgado, Y. Vazquez-Ponce and N. G. Cabo-Bizet by helpful conversations and comments. In addition, the relevant support received from the Proyecto Nacional de Ciencias Básicas (PNCB, CITMA, Cuba) and from the Network N-35 of the Office of External Activities (OEA) of the ASICTP (Italy) are deeply acknowledged.

APPENDIX A: MATRIX ELEMENTS.

1. Brackets notation

The bracket terms in (3) represent the following integrals:

$$\begin{aligned} \langle m | \hat{\mathcal{H}}_0 | p \rangle &\equiv \sum_s \int d^2x \phi_m^*(x, s) \hat{\mathcal{H}}_0(x) \phi_p(x, s), \\ \langle m, n | V | o, p \rangle &\equiv \sum_{s, s'} \int d^2x d^2x' \phi_m^*(x, s) \phi_n^*(x', s') V(x, x') \phi_o(x', s') \phi_p(x, s), \end{aligned} \tag{A1}$$

where m , n , o and p , denote anyone of the possible quantum number arrays.

2. Dimensionless definitions.

Before writing the expressions for the operators matrix elements, we begin by showing some other useful definitions, as for instance the employed dimensionless ones:

$$\tilde{p} \equiv 1 \quad \text{Unit of distance,} \tag{A2}$$

$$\tilde{a} \equiv \frac{a}{p} \quad \text{Dimensionless characteristic length,} \tag{A3}$$

$$\tilde{\mathbf{R}} \equiv \frac{\mathbf{R}}{p} \quad \text{Dimensionless lattice points position,} \tag{A4}$$

$$\tilde{V} \equiv \frac{ma^2}{\hbar^2} V \quad \text{Dimensionless Coulomb potential.} \tag{A5}$$

From those definitions, the used reference conventions can be inferred. That is, the distances are expressed in units of the Cu nearest neighbors separation $p = 3.6 \text{ \AA}$; and the energies and potential interactions, in units of the quantity $\frac{\hbar^2}{ma^2}$, that for the employed parameters is equivalent to 8.3 eV.

3. Other definitions and properties.

We had already defined along the paper the Wannier orbitals $\varphi_{\mathbf{R}^{(r)}}$, as normalized gaussian functions, centered in $\mathbf{R}^{(r)}$ and with characteristic parameter a . In order to simplify notation when the jellium in (7) is going to be used,

is useful to define:

$$\varphi_0^b(\mathbf{x}) = \frac{1}{\sqrt{\pi b^2}} \exp\left(-\frac{\mathbf{x}^2}{2b^2}\right). \quad (\text{A6})$$

Let us use (A6) for defining the jellium's potential

$$F_b(\mathbf{x}) = \sum_{\mathbf{R}} \int d^2y \varphi_{\mathbf{R}}^{b*}(\mathbf{y}) V(\mathbf{x} - \mathbf{y}) \varphi_{\mathbf{R}}^b(\mathbf{y}). \quad (\text{A7})$$

In obtaining the matrix elements of the jellium potential (A7), the following notation is useful:

$$\langle \mathbf{R}^{(r)}, \mathbf{R}^b | V | \mathbf{R}^b, \mathbf{R}^{(t)} \rangle \equiv \int d^2x d^2y \varphi_{\mathbf{R}^{(r)}}^*(\mathbf{x}) \varphi_{\mathbf{R}^{(t)}}^{b*}(\mathbf{y}) V(\mathbf{x} - \mathbf{y}) \varphi_{\mathbf{R}^{(t)}}^b(\mathbf{y}) \varphi_{\mathbf{R}^{(r)}}(\mathbf{x}), \quad (\text{A8})$$

where labels r and t move on the sublattices independently. In the context of the infinite lattice problem is easy to see the following property

$$\langle \mathbf{R}^{(r)}, \mathbf{R}^b | V | \mathbf{R}^b, \mathbf{R}^{(t)} \rangle = \langle \mathbf{R}^{(r)} - \mathbf{R}, \mathbf{0}^b | V | \mathbf{0}^b, \mathbf{R}^{(t)} - \mathbf{R} \rangle, \quad (\text{A9})$$

which can be proved by making a pair of changes of variables on the second order integral in the right hand side of (A8). For finite systems the prove is a little more complicated. Firstly, the integrals extend over the region occupied by the lattice, and for this region the integration does not remain invariant under the translations that must be done. It becomes necessary to periodically extend the Coulomb interaction beyond the boundaries. That is, modified it to the form

$$V_p(\mathbf{x}, \mathbf{y}) = \frac{e^2}{4\pi\epsilon\epsilon_0} \sum_{n_1, n_2} \frac{1}{|\mathbf{x} - \mathbf{y} + n_1 L \hat{\mathbf{e}}_{x_1} + n_2 L \hat{\mathbf{e}}_{x_2}|}, \quad (\text{A10})$$

where n_1 and $n_2 = \dots, -1, 0, 1, \dots$, and L is the length of the side of the squared region which the system occupies. However when the system is sufficiently large, the error done by no extending it periodically is not important; and it vanishes in thermodynamic limit.

Equally useful in defining the direct and exchange potential matrix elements, is the following notation

$$\langle \mathbf{R}^{(r)}, \mathbf{R}^{(t')} | V | \mathbf{R}^{(t'')}, \mathbf{R}^{(t)} \rangle \equiv \int d^2x d^2y \varphi_{\mathbf{R}^{(r)}}^*(\mathbf{x}) \varphi_{\mathbf{R}^{(t')}}^*(\mathbf{y}) V(\mathbf{x} - \mathbf{y}) \varphi_{\mathbf{R}^{(t'')}}(\mathbf{y}) \varphi_{\mathbf{R}^{(t)}}(\mathbf{x}), \quad (\text{A11})$$

where t' and t'' also move on both sublattices independently. In the same manner they fulfill the following property

$$\langle \mathbf{R}^{(r)}, \mathbf{R}^{(t')} | V | \mathbf{R}^{(t'')}, \mathbf{R}^{(t)} \rangle \equiv \langle \mathbf{R}^{(r)} - \mathbf{R}^{(t'')}, \mathbf{R}^{(t')} - \mathbf{R}^{(t'')} | V | \mathbf{0}, \mathbf{R}^{(t)} - \mathbf{R}^{(t'')} \rangle, \quad (\text{A12})$$

if we define

$$\mathbf{R}^{(t', t'')} \equiv \mathbf{R}^{(t')} - \mathbf{R}^{(t'')}. \quad (\text{A13})$$

Then it follows

$$\mathbf{R}^{(t', t'')} = \begin{cases} \mathbf{R}^{(1)}, & \text{if } t' = t'', \\ \mathbf{R}^{(2)}, & \text{if } t' \neq t''. \end{cases} \quad (\text{A14})$$

Let us consider the definitions of $\mathbf{R}^{(1)}$ and $\mathbf{R}^{(2)}$ given in (10), and recall that the only Wannier orbitals which have non vanishing overlapping are those centered on the same site or the ones centered in nearest neighbors (the closest neighbors belong to different sublattice). Then for fixed $\mathbf{R}^{(r)}$ and $\mathbf{R}^{(t)}$, the only no vanishing among all the quantities in the left hand side of (A12) are

$$\langle \mathbf{R}^{(r)} - \mathbf{R}^{(t'')}, \mathbf{0} | V | \mathbf{0}, \mathbf{R}^{(t)} - \mathbf{R}^{(t'')} \rangle \quad \text{for } t' = t'', \quad (\text{A15})$$

and

$$\langle \mathbf{R}^{(r)} - \mathbf{R}^{(t'')}, \mathbf{p}_i | V | \mathbf{0}, \mathbf{R}^{(t)} - \mathbf{R}^{(t'')} \rangle \quad \text{for } t' \neq t'', \quad (\text{A16})$$

in which $i=1, \dots, 4$. The four quantities \mathbf{p}_i are defined as

$$\mathbf{p}_i = \begin{cases} p \hat{\mathbf{e}}_{x_1}, & \text{if } i=1, \\ -p \hat{\mathbf{e}}_{x_1}, & \text{if } i=2, \\ p \hat{\mathbf{e}}_{x_2}, & \text{if } i=3, \\ -p \hat{\mathbf{e}}_{x_2}, & \text{if } i=4. \end{cases} \quad (\text{A17})$$

That is, they move over the neighbors which are closest to the site on the origin.

The employed procedure reduces the number of integrals appearing in (A15), (A16), inclusive those corresponding to the right hand side in (A9) and anyone of those appearing when the matrix elements of the periodic potential W_γ , or the projection of the tight binding Bloch basis between any two elements, are searched. By example

$$\langle \mathbf{R}^{(r)} | W_\gamma | \mathbf{R}^{(t)} \rangle \equiv \int d^2x \varphi_{\mathbf{R}^{(r)}}^* W_\gamma \varphi_{\mathbf{R}^{(t)}}, \quad (\text{A18})$$

$$\langle \mathbf{R}^{(r)} | \mathbf{R}^{(t)} \rangle \equiv \int d^2x \varphi_{\mathbf{R}^{(r)}}^* \varphi_{\mathbf{R}^{(t)}}, \quad (\text{A19})$$

which respectively fulfill the following properties

$$\langle \mathbf{R}^{(r)} | W_\gamma | \mathbf{R}^{(t)} \rangle = \langle \mathbf{R}^{(r,t)} | W_\gamma | \mathbf{0} \rangle, \quad (\text{A20})$$

$$\langle \mathbf{R}^{(r)} | \mathbf{R}^{(t)} \rangle = \langle \mathbf{R}^{(r,t)} | \mathbf{0} \rangle, \quad (\text{A21})$$

given the periodicity of W_γ in the absolute sublattice.

In the following subsection it is frequently used the symbol $\delta_{r,t+1}$ in which $t+1$ is not the usual sum of 1, but the transformation of a given sublattice in another

$$t+1 = \begin{cases} 2 & \text{if } t=1, \\ 1 & \text{if } t=2. \end{cases} \quad (\text{A22})$$

4. Matrix Elements.

Making use of the previously definitions given in this Appendix and after performing an extensive algebraic work, the desired matrix elements are computed. Below we start presenting them:

$$E_{\mathbf{k},(t,\alpha_z),(r,\sigma_z)}^0 = \delta_{\alpha_z,\sigma_z} \left[\widetilde{W}_{00} \delta_{t,r} + 2\widetilde{\gamma}(\cos k_1 p + \cos k_2 p) \delta_{t,r+1} \right], \quad (\text{A23})$$

$$I_{\mathbf{k},(t,\alpha_z),(r,\sigma_z)} = \delta_{\alpha_z,\sigma_z} \left[I_{00} \delta_{t,r} + 2I_{01}(\cos k_1 p + \cos k_2 p) \delta_{t,r+1} \right], \quad (\text{A24})$$

$$F_{\mathbf{k},(t,\alpha_z),(r,\sigma_z)} = \delta_{\alpha_z,\sigma_z} \left[F_{00} \delta_{t,r} + 2F_{01}(\cos k_1 p + \cos k_2 p) \delta_{t,r+1} \right], \quad (\text{A25})$$

where $\widetilde{W}_{00} = 0$, represents a change in the zero point energy; and $\widetilde{\gamma}$ is a free parameter describing our lack of knowledge about the periodic potential. The other appearing parameters are defined as

$$\begin{aligned} I_{00} &= \langle \mathbf{0} | \mathbf{0} \rangle \\ &= 1, \end{aligned} \quad (\text{A26})$$

$$\begin{aligned} I_{01} &= \langle 0 | \widetilde{\mathbf{p}}_1 \rangle \\ &= e^{-\frac{1}{4a^2}}, \end{aligned} \quad (\text{A27})$$

$$F_{00} = \frac{2}{N} \sum_{\widetilde{\mathbf{R}}} \langle \widetilde{\mathbf{R}}, \mathbf{0}^b | \widetilde{V} | \mathbf{0}^b, \widetilde{\mathbf{R}} \rangle, \quad (\text{A28})$$

$$F_{01} = \frac{2}{N} \sum_{\widetilde{\mathbf{R}}} \langle \widetilde{\mathbf{R}} + \widetilde{\mathbf{p}}_1, \mathbf{0}^b | \widetilde{V} | \mathbf{0}^b, \widetilde{\mathbf{R}} \rangle, \quad (\text{A29})$$

where N is the number of electrons in the electron gas and, as we had already defined, the symbol \sim means dimensionless.

The matrix elements of the direct potential are

$$\begin{aligned} G_{\mathbf{k},(t,\alpha_z),(r,\sigma_z)}^{dir} &= \sum_{\mathbf{k}',\mathbf{l}} \Theta_{(\varepsilon_F - \varepsilon_1(\mathbf{k}'))} \delta_{\alpha_z, \sigma_z} \times [\delta_{t,r} B_{(t',\sigma'_z)}^{\mathbf{k}',\mathbf{l}*} \delta_{\sigma'_z, \sigma''_z} (\delta_{t',t''} Z_0^{(t',t'')} + \delta_{t',t''+1} Z_1^{(\mathbf{k}',t',t'')}) B_{(t'',\sigma''_z)}^{\mathbf{k}',\mathbf{l}} \\ &+ \delta_{t,r+1} B_{(t',\sigma'_z)}^{\mathbf{k}',\mathbf{l}*} \delta_{\sigma'_z, \sigma''_z} (\delta_{t',t''} Z_1^{(\mathbf{k}',t',t'')} + \delta_{t',t''+1} Z_3^{(\mathbf{k},\mathbf{k}',t',t'')}) B_{(t'',\sigma''_z)}^{\mathbf{k}',\mathbf{l}}], \end{aligned} \quad (\text{A30})$$

where

$$Z_0^{(t',t'')} \equiv \frac{2}{N} \sum_{\widetilde{\mathbf{R}}^{(t',t'')}} \langle \widetilde{\mathbf{R}}^{(t',t'')}, \mathbf{0} | \widetilde{V} | \mathbf{0}, \widetilde{\mathbf{R}}^{(t',t'')} \rangle, \quad (\text{A31})$$

$$Z_1^{(\mathbf{k},t',t'')} \equiv \frac{2}{N} \sum_i \sum_{\widetilde{\mathbf{R}}^{(t',t'')}} \cos(\mathbf{k} \cdot \mathbf{p}_i) \langle \widetilde{\mathbf{p}}_i + \widetilde{\mathbf{R}}^{(t',t'')}, \mathbf{0} | \widetilde{V} | \mathbf{0}, \widetilde{\mathbf{R}}^{(t',t'')} \rangle, \quad (\text{A32})$$

$$Z_3^{(\mathbf{k},\mathbf{k}',t',t'')} \equiv \frac{2}{N} \sum_{i,j} \sum_{\widetilde{\mathbf{R}}^{(t',t'')}} \cos(\mathbf{k} \cdot \mathbf{p}_i + \mathbf{k}' \cdot \mathbf{p}_j) \langle \widetilde{\mathbf{p}}_i + \widetilde{\mathbf{R}}^{(t',t'')}, \widetilde{\mathbf{p}}_j | \widetilde{V} | \mathbf{0}, \widetilde{\mathbf{R}}^{(t',t'')} \rangle. \quad (\text{A33})$$

For simplicity, in expression (A30) the Einstein summation convention for the indices $(t', t'', \sigma'_z, \sigma''_z)$ is employed. Further, the matrix elements of the exchange potential are

$$\begin{aligned} G_{\mathbf{k},(t,\alpha_z),(r,\sigma_z)}^{ind} &= \sum_{\mathbf{k}',\mathbf{l}} \Theta_{(\varepsilon_F - \varepsilon_1(\mathbf{k}'))} \times [B_{(r,\sigma_z)}^{\mathbf{k}',\mathbf{l}*} S_0^{(\mathbf{k},\mathbf{k}',t,r)} B_{(t,\alpha_z)}^{\mathbf{k}',\mathbf{l}} + B_{(r,\sigma_z)}^{\mathbf{k}',\mathbf{l}*} S_1^{(\mathbf{k},\mathbf{k}',t,r+1)} B_{(t+1,\alpha_z)}^{\mathbf{k}',\mathbf{l}} \\ &+ B_{(r+1,\sigma_z)}^{\mathbf{k}',\mathbf{l}*} S_1^{(\mathbf{k},\mathbf{k}',t+1,r)} B_{(t,\alpha_z)}^{\mathbf{k}',\mathbf{l}} + B_{(r+1,\sigma_z)}^{\mathbf{k}',\mathbf{l}*} S_3^{(\mathbf{k},\mathbf{k}',t,r)} B_{(t+1,\alpha_z)}^{\mathbf{k}',\mathbf{l}}], \end{aligned} \quad (\text{A34})$$

where

$$S_0^{(\mathbf{k},\mathbf{k}',t',t'')} = \frac{2}{N} \sum_{\widetilde{\mathbf{R}}^{(t',t'')}} \cos[(\mathbf{k} - \mathbf{k}') \cdot \widetilde{\mathbf{R}}^{(t',t'')}] \times \langle \widetilde{\mathbf{R}}^{(t',t'')}, \mathbf{0} | \widetilde{V} | \mathbf{0}, \widetilde{\mathbf{R}}^{(t',t'')} \rangle, \quad (\text{A35})$$

$$S_1^{(\mathbf{k},\mathbf{k}',t',t'')} = \frac{2}{N} \sum_i \sum_{\widetilde{\mathbf{R}}^{(t',t'')}} \cos[\mathbf{k} \cdot \mathbf{p}_i + (\mathbf{k} - \mathbf{k}') \cdot \widetilde{\mathbf{R}}^{(t',t'')}] \times \langle \widetilde{\mathbf{p}}_i + \widetilde{\mathbf{R}}^{(t',t'')}, \mathbf{0} | \widetilde{V} | \mathbf{0}, \widetilde{\mathbf{R}}^{(t',t'')} \rangle, \quad (\text{A36})$$

$$S_3^{(\mathbf{k},\mathbf{k}',t',t'')} = \frac{2}{N} \sum_{i,j} \sum_{\widetilde{\mathbf{R}}^{(t',t'')}} \cos[\mathbf{k} \cdot (\mathbf{p}_i + \mathbf{p}_j) + (\mathbf{k} - \mathbf{k}') \cdot \widetilde{\mathbf{R}}^{(t',t'')}] \times \langle \widetilde{\mathbf{p}}_i + \widetilde{\mathbf{R}}^{(t',t'')}, \widetilde{\mathbf{p}}_j | \widetilde{V} | \mathbf{0}, \widetilde{\mathbf{R}}^{(t',t'')} \rangle. \quad (\text{A37})$$

5. Reducing the order of some integrals.

Any one of the fourth fold integrals presented in previous sections, can be partially integrated in quadratures, in such a way they final calculation is reduced to numerically evaluate first order integrals. Thus

$$\begin{aligned} \langle \tilde{\mathbf{R}} + \tilde{\mathbf{p}}_1, \tilde{\mathbf{p}}_3 | \tilde{V} | \mathbf{0}, \tilde{\mathbf{R}} \rangle &= \frac{\exp[-\frac{1}{2\tilde{a}^2}]}{2\sqrt{2\pi\tilde{a}^2}} \times \int_0^{2\pi} d\phi \exp\left\{-\frac{[(\tilde{R}_{x_1} + \frac{1}{2}) \sin \phi - (\tilde{R}_{x_2} - \frac{1}{2}) \cos \phi]^2}{2\tilde{a}^2}\right\} \\ &\times \text{Erfc}\left\{-\frac{[(\tilde{R}_{x_2} - \frac{1}{2}) \sin \phi - (\tilde{R}_{x_1} + \frac{1}{2}) \cos \phi]^2}{2\tilde{a}^2}\right\}, \end{aligned} \quad (\text{A38})$$

where Erfc is the complement error function. Similarly

$$\begin{aligned} \langle \tilde{\mathbf{R}} + \tilde{\mathbf{p}}_1, \mathbf{0}^b | \tilde{V} | \mathbf{0}^b, \tilde{\mathbf{R}} \rangle &= \frac{\exp[-\frac{1}{4\tilde{a}^2}]}{\sqrt{\frac{4(1+\zeta^2)\pi\tilde{a}^2}{\zeta^2}}} \times \int_0^{2\pi} d\phi \exp\left\{-\frac{[(\tilde{R}_{x_1} + \frac{1}{2}) \sin \phi - \tilde{R}_{x_2} \cos \phi]^2}{\frac{(1+\zeta^2)\tilde{a}^2}{\zeta^2}}\right\} \\ &\times \text{Erfc}\left\{-\frac{[\tilde{R}_{x_2} \sin \phi - (\tilde{R}_{x_1} + \frac{1}{2}) \cos \phi]^2}{\frac{(1+\zeta^2)\tilde{a}^2}{\zeta^2}}\right\}, \end{aligned} \quad (\text{A39})$$

where $\zeta \equiv \frac{a}{b}$.

-
- ¹ N. F. Mott, Proc. Phys. Soc. A62, 416, (1949).
 - ² J. C. Slater, Phys. Rev. 81, 385, (1951).
 - ³ R. Peierls, Proc. Phys. Soc. A49, 72 (1937).
 - ⁴ F. Hubbard, Proc. R. Soc. A276, 238 (1963).
 - ⁵ P. W. Anderson, Science 235, 1196, (1987).
 - ⁶ P. W. Anderson, Phys. Rev.115, 2 (1959).
 - ⁷ W. Kohn, Phys. Rev. A171, 133 (1964).
 - ⁸ W. F. Brinkman and T. M. Rice, Phys. Rev.B2, 4302, (1970).
 - ⁹ M. Gutzwiller, Phys. Rev. A134, 923 (1964).
 - ¹⁰ M. Gutzwiller, Phys. Rev. A137, 1726 (1965).
 - ¹¹ M. Imada, Rev. Mod. Phys. 70,4 (1998).
 - ¹² E. Dagotto, Rev. Mod. Phys. 66, 763 (1994).
 - ¹³ Y. Yanase, Phys. Rep. 387, 1 (2003).
 - ¹⁴ D. J. Van Harlingen, Rev. Mod. Phys. 67, 515 (1995).
 - ¹⁵ A. Damascelli, Rev. Mod. Phys. 75, (2003).
 - ¹⁶ J. G. Bednorz and K. A. Müller, Rev. Mod. Phys. 60, 585 (1987).
 - ¹⁷ G. Burns, *High-Temperature Superconductivity*, Academic Press, New York (1992).
 - ¹⁸ C. Almasan and M. B. Maple, *Chemistry of High Temperature Superconductors*, World Scientific, Singapore (1991).
 - ¹⁹ N. F. Mott, *Metal-Insulator Transition*, Taylor and Francis, London, Philadelphia (1990).
 - ²⁰ E. Fradkin, *Field Theories of Condensed Matter*, Addison Wesley Publishing Company (1991).
 - ²¹ K. Terakura, A. R. Williams, T. Oguchi and J. Kubler, Phys. Rev. Lett. 52, 1830 (1984).
 - ²² L. F. Mattheiss, Phys. Rev. Lett. 58, 1028 (1987).
 - ²³ W. Kohn and L. J. Sham, Phys. Rev. A140, 1133 (1965).
 - ²⁴ P. A. M. Dirac, Proc. Cambridge. Phil. Soc. 26, 376 (1930).
 - ²⁵ J. C. Slater, *Quantum Theory of Atomic Structure*, Dover Publications Inc., Mineola, New York., v. 2 (1960).
 - ²⁶ W. E. Pickett, Rev. Mod. Phys. 61, 2 (1999).
 - ²⁷ C. Yannouleas and U. Landman, Phys. Rev. Lett. 82, 5325 (1999).
 - ²⁸ A. Szabo and N. Ostlund, *Modern Quantum Chemistry: Introduction to Advanced Electronic Structure Theory*, Dover Publications Inc., Mineola, New York (1989).
 - ²⁹ A. L. Fetter and J. D. Walecka, *Quantum Theory of Many Particle Physics*, McGraw-Hill, Inc. (1971).
 - ³⁰ Y. V. Ponce, D. Oliva and A. Cabo, Phys. Lett. A353, 255 (2006).